

**Stereochemically Controlled Synthesis of Ruthenium(II) Complexes Containing Bis(oxazolin-2'-yl)pyridine Ligands. X-ray Crystal Structures of *trans*-[RuCl<sub>2</sub>(PPh<sub>3</sub>)<sub>2</sub>{κ<sup>3</sup>-*N,N,N*-(*S,S*)-<sup>i</sup>Pr-pybox}] and [RuCl(=C=C=CPh<sub>2</sub>)(PPh<sub>3</sub>)<sub>2</sub>{κ<sup>3</sup>-*N,N,N*-(*S,S*)-<sup>i</sup>Pr-pybox}][PF<sub>6</sub>] ((*S,S*)-<sup>i</sup>Pr-pybox = 2,6-Bis[4'-(*S*)-isopropylloxazolin-2'-yl]pyridine)**

Victorio Cadierno, M. Pilar Gamasa, José Gimeno,\* and Luis Iglesias

Departamento de Química Orgánica e Inorgánica, Instituto Universitario de Química Organometálica "Enrique Moles" (Unidad Asociada al CSIC), Universidad de Oviedo, E-33071 Oviedo, Spain

Santiago García-Granda

Departamento de Química Física y Analítica, Universidad de Oviedo, E-33071 Oviedo, Spain

Received November 17, 1998

The treatment of achiral and chiral bis(oxazolin-2'-yl)pyridine (pybox) complexes *trans*-[RuCl<sub>2</sub>(η<sup>2</sup>-H<sub>2</sub>C=CH<sub>2</sub>)-(κ<sup>3</sup>-*N,N,N*-pybox)] [pybox = 2,6-bis(dihydrooxazolin-2'-yl)pyridine] (**1a**) and [RuCl<sub>2</sub>(η<sup>2</sup>-H<sub>2</sub>C=CH<sub>2</sub>)(κ<sup>3</sup>-*N,N,N*-(*SS*)-<sup>i</sup>Pr-pybox)] [(*SS*)-<sup>i</sup>Pr-pybox = 2,6-bis[4'-(*S*)-isopropylloxazolin-2'-yl]pyridine] (**1b**) with an excess of triphenylphosphine in dichloromethane at 50 °C leads to the formation of the first ruthenium(II) derivatives containing both bis(oxazolin-2'-yl)pyridine and phosphine ligands *trans*-[RuCl<sub>2</sub>(PPh<sub>3</sub>)<sub>2</sub>(κ<sup>3</sup>-*N,N,N*-pybox)] (**2a**) and *trans*-[RuCl<sub>2</sub>(PPh<sub>3</sub>)<sub>2</sub>(κ<sup>3</sup>-*N,N,N*-(*SS*)-<sup>i</sup>Pr-pybox)] (**2b**). Chiral complex **2b** slowly isomerizes in acetone at 50 °C to generate *cis*-[RuCl<sub>2</sub>(PPh<sub>3</sub>)<sub>2</sub>(κ<sup>3</sup>-*N,N,N*-(*SS*)-<sup>i</sup>Pr-pybox)] (**3**). Complex **3** can be also obtained from the reaction of **1b** with PPh<sub>3</sub> in MeOH. The structure of **3** has been confirmed by X-ray crystallography [orthorhombic; space group *P*2<sub>1</sub>2<sub>1</sub>2<sub>1</sub>; *Z* = 4; *a* = 12.772(6) Å, *b* = 15.208(5) Å, *c* = 19.601(7) Å; final *R*<sub>1</sub> = 0.0565 and *wR*<sub>2</sub> = 0.0944 (both for *I* > 2σ(*I*)). The reaction of the achiral pybox complex **2a** with 1,1-diphenyl-2-propyn-1-ol and AgBF<sub>4</sub> in CH<sub>2</sub>Cl<sub>2</sub> stereoselectively affords the cationic allenylidene derivative [RuCl(=C=C=CPh<sub>2</sub>)(PPh<sub>3</sub>)<sub>2</sub>(κ<sup>3</sup>-*N,N,N*-pybox)][BF<sub>4</sub>] (**4a**), while the methoxycarbene complex [RuCl(=C(OMe)CH=CPh<sub>2</sub>)(PPh<sub>3</sub>)<sub>2</sub>(κ<sup>3</sup>-*N,N,N*-pybox)][PF<sub>6</sub>] (**5**) is obtained when the reaction is conducted in methanol and in the presence of NaPF<sub>6</sub>, via the addition of MeOH to the initially formed allenylidene complex **4a**. In contrast, the chiral pybox complex **2b** reacts with 1,1-diphenyl-2-propyn-1-ol and NaPF<sub>6</sub> in MeOH to give the stable allenylidene complex [RuCl(=C=C=CPh<sub>2</sub>)(PPh<sub>3</sub>)<sub>2</sub>(κ<sup>3</sup>-*N,N,N*-(*SS*)-<sup>i</sup>Pr-pybox)][PF<sub>6</sub>] (**4b**). The X-ray crystal structure of **4b** [orthorhombic; space group *P*2<sub>1</sub>2<sub>1</sub>2<sub>1</sub>; *Z* = 4; *a* = 14.79(3) Å, *b* = 16.254(8) Å, *c* = 22.917(18) Å; final *R*<sub>1</sub> = 0.0545 and *wR*<sub>2</sub> = 0.1381 (both for *I* > 2σ(*I*))] shows an octahedral coordination of the ligands around the ruthenium atom with the chloride and triphenylphosphine ligands in a *trans* arrangement and mutually *cis* with respect to the allenylidene moiety. The allenylidene complex **4b** is also formed by the reaction of the *cis* dichloride complex **3** with 1,1-diphenyl-2-propyn-1-ol and NaPF<sub>6</sub> in MeOH. IR, <sup>1</sup>H, <sup>31</sup>P{<sup>1</sup>H}, and <sup>13</sup>C{<sup>1</sup>H} NMR data of all novel compounds are also reported.

## Introduction

Over the last two decades, chiral bidentate bis(oxazoline) ligands have attracted much attention as useful auxiliaries in transition-metal-mediated enantioselective transformations.<sup>1</sup> An interesting new class of related chiral ligands are the C<sub>2</sub>-symmetric terdentate bis(oxazoline) ligands, such as 2,6-bis[4'-(*R* or *S*)-alkyloxazolin-2'-yl]pyridine [(*RR* or *SS*)-*R*-pybox], prepared by Nishiyama et al.<sup>2</sup> Successful applications for the

enantiocontrol of several processes catalyzed by transition-metal pybox complexes have been recently reported.<sup>1–3</sup> In particular, the ruthenium(II) complex *trans*-[RuCl<sub>2</sub>(η<sup>2</sup>-H<sub>2</sub>C=CH<sub>2</sub>){κ<sup>3</sup>-*N,N,N*-(*SS*)-<sup>i</sup>Pr-pybox}] [(*SS*)-<sup>i</sup>Pr-pybox = 2,6-bis[4'-(*S*)-isopropylloxazolin-2'-yl]pyridine] has been used as an efficient catalyst for the asymmetric cyclopropanation of olefins.<sup>3</sup> Despite the interest in such ruthenium(II) pybox derivatives, its chemistry has been only partially investigated,<sup>3,4</sup> and quantification of the steric and electronic effects of the oxazoline-ring substituents on the chemical behavior of these complexes has not yet been explored. Here we report the stereochemically

\* Corresponding author. E-mail: jgh@sauron.quimica.uniovi.es.

- (1) For reviews, see: (a) Pfaltz, A. *Acc. Chem. Res.* **1993**, *26*, 339–345. (b) Pfaltz, A. *Acta Chem. Scand.* **1996**, *50*, 189–194. (c) Trost, B. M.; Van Vranken, D. L. *Chem. Rev.* **1996**, *96*, 395–422. (d) Ager, D. J.; Prakash, I.; Schaad, D. R. *Chem. Rev.* **1996**, *96*, 835–875. (e) Ghosh, A. K.; Mathivanan, P.; Cappiello, J. *Tetrahedron* **1998**, *9*, 1. (2) Nishiyama, H.; Kondo, M.; Nakamura, T.; Itoh, K. *Organometallics* **1991**, *10*, 500–508.

- (3) (a) Nishiyama, H.; Itoh, Y.; Matsumoto, H.; Park, S. B.; Itoh, K. *J. Am. Chem. Soc.* **1994**, *116*, 2223–2224 and references therein. (b) Nishiyama, H.; Itoh, Y.; Sugawara, Y.; Matsumoto, H.; Aoki, K.; Itoh, K. *Bull. Chem. Soc. Jpn.* **1995**, *68*, 1247–1262. (c) Park, S.-B.; Sakata, N.; Nishiyama, H. *Chem. Eur. J.* **1996**, *2*, 303–306.

controlled synthesis of the first ruthenium(II) complexes containing both chiral and achiral bis(oxazolin-2'-yl)pyridine and phosphine ligands: *trans*-[RuCl<sub>2</sub>(PPh<sub>3</sub>)(κ<sup>3</sup>-N,N,N-pybox)] [pybox = 2,6-bis(dihydrooxazolin-2'-yl)pyridine] (**2a**), *trans*-[RuCl<sub>2</sub>(PPh<sub>3</sub>){κ<sup>3</sup>-N,N,N-(SS)-iPr-pybox}] (**2b**), and *cis*-[RuCl<sub>2</sub>(PPh<sub>3</sub>){κ<sup>3</sup>-N,N,N-(SS)-iPr-pybox}] (**3**). In addition, the preparation of novel allenylidene complexes [RuCl(=C=C=CPh<sub>2</sub>)(PPh<sub>3</sub>)(κ<sup>3</sup>-N,N,N-pybox)][BF<sub>4</sub>] (**4a**), [RuCl(=C=C=CPh<sub>2</sub>)(PPh<sub>3</sub>){κ<sup>3</sup>-N,N,N-(SS)-iPr-pybox}][PF<sub>6</sub>] (**4b**), and the methoxyalkenyl carbene complex [RuCl(=C(OMe)CH=CPh<sub>2</sub>)(PPh<sub>3</sub>)(κ<sup>3</sup>-N,N,N-pybox)][PF<sub>6</sub>] (**5**) is also described.

## Experimental Section

The manipulations were performed under an atmosphere of dry nitrogen using vacuum-line and standard Schlenk techniques. All reagents were obtained from commercial suppliers and used without further purification. Solvents were dried by standard methods and distilled under nitrogen before use. The compounds *trans*-[RuCl<sub>2</sub>(η<sup>2</sup>-H<sub>2</sub>C=CH<sub>2</sub>)(κ<sup>3</sup>-N,N,N-pybox)] (**1a**)<sup>3b</sup> and *trans*-[RuCl<sub>2</sub>(η<sup>2</sup>-H<sub>2</sub>C=CH<sub>2</sub>)(κ<sup>3</sup>-N,N,N-(SS)-iPr-pybox)] (**1b**)<sup>3a</sup> were prepared by following the methods reported in the literature. Infrared spectra were recorded on a Perkin-Elmer 1720-XFT spectrometer. The conductivities were measured at room temperature, in ca. 10<sup>-3</sup> mol dm<sup>-3</sup> acetone solutions, with a Jenway PDM3 conductimeter. The C, H, and N analyses were carried out with a Perkin-Elmer 240-B microanalyzer. NMR spectra were recorded on a Bruker AC300 instrument at 300 MHz (<sup>1</sup>H), 121.5 MHz (<sup>31</sup>P), or 75.4 MHz (<sup>13</sup>C) using SiMe<sub>4</sub> or 85% H<sub>3</sub>PO<sub>4</sub> as standards. DEPT experiments have been carried out for all the complexes (abbreviations used: s, singlet; d, doublet; t, triplet; m, multiplet).

**Synthesis of Complex *trans*-[RuCl<sub>2</sub>(PPh<sub>3</sub>)(κ<sup>3</sup>-N,N,N-pybox)] (**2a**).** A solution of *trans*-[RuCl<sub>2</sub>(η<sup>2</sup>-H<sub>2</sub>C=CH<sub>2</sub>)(κ<sup>3</sup>-N,N,N-pybox)] (**1a**) (0.417 g, 1 mmol) and triphenylphosphine (1.311 g, 5 mmol) in 30 mL of dichloromethane was heated at 50 °C in a sealed tube for 12 h. A change of color from red to violet was observed. The solvent was then concentrated to ca. 5 mL, and the residue transferred to a silica gel chromatography column. Elution with a mixture dichloromethane/methanol (100/1) gave a violet band from which complex **2a** was isolated by solvent removal. Yield 69% (0.449 g). Anal. Calcd for RuC<sub>29</sub>H<sub>26</sub>N<sub>3</sub>Cl<sub>2</sub>O<sub>2</sub>P: C, 53.46; H, 4.02; N, 6.45. Found: C, 53.10; H, 4.23; N, 5.83. <sup>31</sup>P{<sup>1</sup>H} NMR (CDCl<sub>3</sub>) δ 46.48 (s) ppm; <sup>1</sup>H NMR (CDCl<sub>3</sub>) δ 3.47 and 4.72 (t, 4H each one, J<sub>HH</sub> = 9.8 Hz, CH<sub>2</sub>), 7.35–7.97 (m, 18H, Ph and C<sub>5</sub>H<sub>3</sub>N) ppm; <sup>13</sup>C{<sup>1</sup>H} NMR (CDCl<sub>3</sub>) δ 54.02 (s, NCH<sub>2</sub>), 71.01 (s, OCH<sub>2</sub>), 122.64 and 134.57 (s, CH of C<sub>5</sub>H<sub>3</sub>N), 127.63 (d, <sup>3</sup>J<sub>CP</sub> = 8.4 Hz, *m*-PPh<sub>3</sub>), 129.21 (s, *p*-PPh<sub>3</sub>), 134.78 (d, <sup>2</sup>J<sub>CP</sub> = 9.9 Hz, *o*-PPh<sub>3</sub>), 136.49 (d, J<sub>CP</sub> = 37.6 Hz, *i*-PPh<sub>3</sub>), 148.59 and 166.61 (s, C of C<sub>5</sub>H<sub>3</sub>N and C=NCH<sub>2</sub>) ppm.

**Synthesis of Complex *trans*-[RuCl<sub>2</sub>(PPh<sub>3</sub>){κ<sup>3</sup>-N,N,N-(SS)-iPr-pybox}] (**2b**).** A solution of *trans*-[RuCl<sub>2</sub>(η<sup>2</sup>-H<sub>2</sub>C=CH<sub>2</sub>){κ<sup>3</sup>-N,N,N-(SS)-iPr-pybox}] (**1b**) (0.501 g, 1 mmol) and triphenylphosphine (1.311 g, 5 mmol) in 30 mL of dichloromethane was heated at 50 °C in a sealed tube for 1 h. A change of color from red to violet was observed. The solvent was then concentrated to ca. 5 mL and the residue transferred to a silica gel chromatography column. Elution with a mixture dichloromethane/methanol (100/1) gave a violet band from which complex **2b** was isolated by solvent removal. Yield 64% (0.471 g). Anal. Calcd for RuC<sub>33</sub>H<sub>38</sub>N<sub>3</sub>Cl<sub>2</sub>O<sub>2</sub>P·CH<sub>2</sub>Cl<sub>2</sub>: C, 55.07; H, 5.13; N, 5.35. Found: C, 55.01; H, 5.51; N, 5.16. <sup>31</sup>P{<sup>1</sup>H} NMR (CDCl<sub>3</sub>) δ 38.11 (s) ppm; <sup>1</sup>H NMR (CDCl<sub>3</sub>) δ 0.30 (d, 6H, J<sub>HH</sub> = 7.1 Hz, Me), 0.55 (d, 6H, J<sub>HH</sub> = 6.6 Hz, Me), 1.52 (m, 2H, CHMe<sub>2</sub>), 3.57 (m, 2H, CHPr), 4.51 (m, 4H, CH<sub>2</sub>), 7.33–8.01 (m, 18H, Ph and C<sub>5</sub>H<sub>3</sub>N) ppm; <sup>13</sup>C{<sup>1</sup>H} NMR (CDCl<sub>3</sub>) δ 14.60 and 19.12 (s, Me), 27.92 (s, CHMe<sub>2</sub>), 70.21 (s, CH<sub>2</sub>), 70.57 (s, NCH), 122.98 and 134.20 (s, CH of C<sub>5</sub>H<sub>3</sub>N), 127.39

(d, <sup>3</sup>J<sub>CP</sub> = 8.5 Hz, *m*-PPh<sub>3</sub>), 128.91 (s, *p*-PPh<sub>3</sub>), 134.95 (d, <sup>2</sup>J<sub>CP</sub> = 9.6 Hz, *o*-PPh<sub>3</sub>), 137.30 (d, J<sub>CP</sub> = 35.4 Hz, *i*-PPh<sub>3</sub>), 149.05 and 165.15 (s, C of C<sub>5</sub>H<sub>3</sub>N and C=NCH<sup>i</sup>Pr) ppm.

**Synthesis of Complex *cis*-[RuCl<sub>2</sub>(PPh<sub>3</sub>){κ<sup>3</sup>-N,N,N-(SS)-iPr-pybox}] (**3**).** A solution of *trans*-[RuCl<sub>2</sub>(η<sup>2</sup>-H<sub>2</sub>C=CH<sub>2</sub>){κ<sup>3</sup>-N,N,N-(SS)-iPr-pybox}] (**1b**) (0.501 g, 1 mmol) and triphenylphosphine (1.311 g, 5 mmol) in 30 mL of methanol was heated at 50 °C for 1 h. The solvent was then evaporated in vacuo, and the resulting solid residue was dissolved in dichloromethane (ca. 5 mL) and transferred to a silica gel chromatography column. Elution with a mixture dichloromethane/methanol (10/1) gave a red band from which complex **3** was isolated after solvent removal. Yield 76% (0.559 g). Anal. Calcd for RuC<sub>35</sub>H<sub>38</sub>N<sub>3</sub>Cl<sub>2</sub>O<sub>2</sub>P: C, 57.14; H, 5.20; N, 5.71. Found: C, 56.47; H, 5.64; N, 5.16. <sup>31</sup>P{<sup>1</sup>H} NMR (CDCl<sub>3</sub>) δ 35.34 (s) ppm; <sup>1</sup>H NMR (CDCl<sub>3</sub>) δ -0.12 (d, 3H, J<sub>HH</sub> = 6.6 Hz, Me), 0.79 (d, 3H, J<sub>HH</sub> = 7.0 Hz, Me), 0.89 (d, 3H, J<sub>HH</sub> = 7.2 Hz, Me), 0.96 (d, 3H, J<sub>HH</sub> = 6.6 Hz, Me), 2.40 and 3.02 (m, 1H each one, CHMe<sub>2</sub>), 3.93 and 4.24 (m, 1H each one, CHPr), 4.40–4.69 (m, 4H, CH<sub>2</sub>), 6.98–7.78 (m, 18H, Ph and C<sub>5</sub>H<sub>3</sub>N) ppm; <sup>13</sup>C{<sup>1</sup>H} NMR (CDCl<sub>3</sub>) δ 13.49, 15.50, 19.92 and 20.26 (s, Me), 27.92 and 28.71 (s, CHMe<sub>2</sub>), 69.45 and 69.99 (s, NCH), 70.80 and 71.75 (s, CH<sub>2</sub>), 123.33, 123.87, and 128.43 (s, CH of C<sub>5</sub>H<sub>3</sub>N), 127.95 (d, <sup>3</sup>J<sub>CP</sub> = 9.2 Hz, *m*-PPh<sub>3</sub>), 128.98 (s, *p*-PPh<sub>3</sub>), 132.59 (d, <sup>2</sup>J<sub>CP</sub> = 9.4 Hz, *o*-PPh<sub>3</sub>), 133.58 (d, J<sub>CP</sub> = 41.2 Hz, *i*-PPh<sub>3</sub>), 151.46, 151.77, 165.97, and 167.33 (s, C of C<sub>5</sub>H<sub>3</sub>N and C=NCH<sup>i</sup>Pr) ppm.

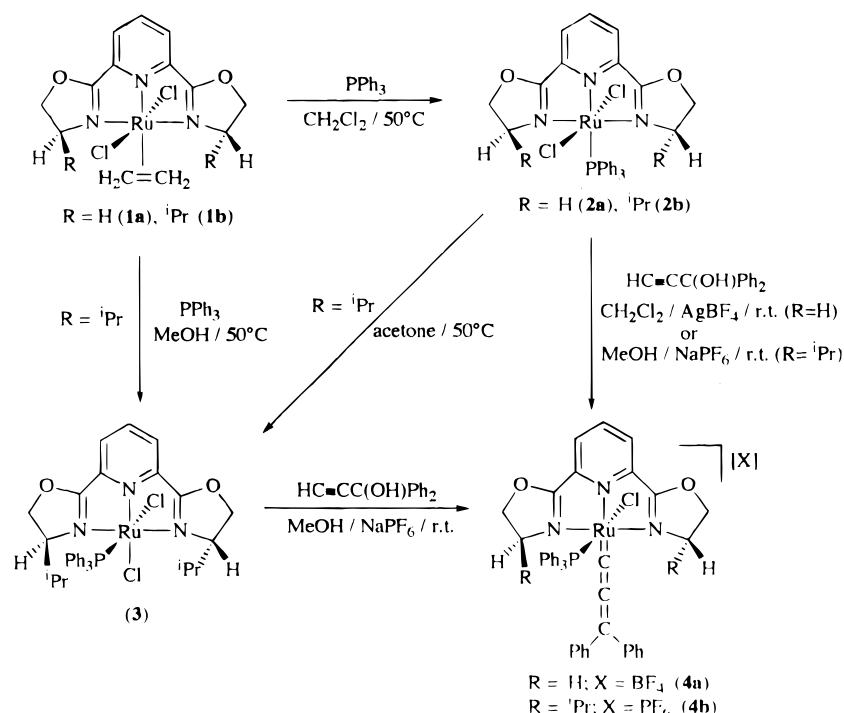
**Synthesis of Complex [RuCl(=C=C=CPh<sub>2</sub>)(PPh<sub>3</sub>)(κ<sup>3</sup>-N,N,N-pybox)][BF<sub>4</sub>] (**4a**).** A mixture of *trans*-[RuCl<sub>2</sub>(PPh<sub>3</sub>)(κ<sup>3</sup>-N,N,N-pybox)] (**2a**) (0.651 g, 1 mmol) and AgBF<sub>4</sub> (0.389 g, 2 mmol) in 35 mL of dichloromethane was stirred at room temperature and in the dark for 15 min. A change of color from violet to red was observed. The suspension was then filtered, and HC≡CC(OH)Ph<sub>2</sub> (1.040 g, 5 mmol) was added to the resulting solution. The reaction mixture was stirred at room temperature for 15 min. The solvent was then concentrated to ca. 5 mL, and 25 mL of a mixture hexane/diethyl ether (3/2) were added yielding a red solid which was washed with diethyl ether (3 × 20 mL) and vacuum-dried. Yield 77% (0.712 g). Anal. Calcd for RuC<sub>44</sub>H<sub>36</sub>F<sub>4</sub>N<sub>3</sub>O<sub>2</sub>BCIP: C, 59.17; H, 4.06; N, 4.70. Found C, 59.21; H, 4.64; N, 5.01. IR (KBr, cm<sup>-1</sup>) ν 1040 (BF<sub>4</sub><sup>-</sup>), 1942 (C=C=C). Conductivity (acetone, 20 °C; Ω<sup>-1</sup> cm<sup>2</sup> mol<sup>-1</sup>) 114. <sup>31</sup>P{<sup>1</sup>H} NMR (CDCl<sub>3</sub>) δ 44.50 (s) ppm; <sup>1</sup>H NMR (CDCl<sub>3</sub>) δ 3.62 and 3.86 (m, 2H each one, OCH<sub>2</sub>), 4.63 and 4.79 (m, 2H each one, NCH<sub>2</sub>), 7.12–8.29 (m, 28H, Ph and C<sub>5</sub>H<sub>3</sub>N) ppm; <sup>13</sup>C{<sup>1</sup>H} NMR (CDCl<sub>3</sub>) δ 54.97 (s, NCH<sub>2</sub>), 72.55 (s, OCH<sub>2</sub>), 125.45 and 131.35 (s, CH of C<sub>5</sub>H<sub>3</sub>N), 127.71–140.31 (m, Ph), 141.62 and 164.91 (s, C of C<sub>5</sub>H<sub>3</sub>N and C=NCH<sup>i</sup>Pr), 143.03 (s, C<sub>ipso</sub> of CPh<sub>2</sub>), 153.88 (s, C<sub>γ</sub>), 205.34 (s, C<sub>β</sub>), 306.59 (d, <sup>2</sup>J<sub>CP</sub> = 22.2 Hz, Ru=C<sub>α</sub>) ppm.

**Synthesis of Complex [RuCl(=C=C=CPh<sub>2</sub>)(PPh<sub>3</sub>){κ<sup>3</sup>-N,N,N-(SS)-iPr-pybox}][PF<sub>6</sub>] (**4b**).** A solution of **2b** or **3** (0.736 g, 1 mmol), NaPF<sub>6</sub> (0.336 g, 2 mmol) and HC≡CC(OH)Ph<sub>2</sub> (0.417 g, 2 mmol) in 50 mL of MeOH was stirred at room temperature for 12 h. The solvent was then removed under vacuum, and the solid residue was extracted with dichloromethane and filtered. The resulting solution was then concentrated to ca. 5 mL, and 100 mL of diethyl ether was added, yielding a red solid which was washed with diethyl ether (3 × 20 mL) and vacuum-dried. Yield 61% (0.631 g). Anal. Calcd for RuC<sub>50</sub>H<sub>48</sub>F<sub>6</sub>N<sub>3</sub>P<sub>2</sub>O<sub>2</sub>Cl·THF: C, 58.56; H, 5.09; N, 3.79. Found: C, 59.19; H, 5.39; N, 3.59. IR (KBr, cm<sup>-1</sup>) ν 840 (PF<sub>6</sub><sup>-</sup>), 1942 (C=C=C). Conductivity (acetone 20 °C; Ω<sup>-1</sup> cm<sup>2</sup> mol<sup>-1</sup>) 126. <sup>31</sup>P{<sup>1</sup>H} NMR (CDCl<sub>3</sub>) δ 38.19 (s) ppm; <sup>1</sup>H NMR (CDCl<sub>3</sub>) δ -0.23 (d, 3H, J<sub>HH</sub> = 6.3 Hz, Me), 0.55 (d, 3H, J<sub>HH</sub> = 6.7 Hz, Me), 0.73 (d, 3H, J<sub>HH</sub> = 6.9 Hz, Me), 0.84 (d, 3H, J<sub>HH</sub> = 6.3 Hz, Me), 2.20 and 3.55 (m, 1H each one, CHMe<sub>2</sub>), 4.08 and 4.39 (m, 1H each one, CHPr), 4.42–4.71 (m, 4H, CH<sub>2</sub>), 7.14–8.29 (m, 28H, Ph and C<sub>5</sub>H<sub>3</sub>N) ppm; <sup>13</sup>C{<sup>1</sup>H} NMR (CDCl<sub>3</sub>) δ 13.42, 15.19, 19.33, and 19.54 (s, Me), 28.37 and 29.39 (s, CHMe<sub>2</sub>), 70.37 and 73.45 (s, NCH), 71.72 and 72.44 (s, CH<sub>2</sub>), 125.61, 125.86, and 131.49 (s, CH of C<sub>5</sub>H<sub>3</sub>N), 128.63–140.36 (m, Ph), 141.92, 142.54, 163.26, and 165.15 (s, C of C<sub>5</sub>H<sub>3</sub>N and C=NCH<sup>i</sup>Pr), 143.43 (s, C<sub>ipso</sub> of CPh<sub>2</sub>), 153.35 (s, C<sub>γ</sub>), 207.34 (s, C<sub>β</sub>), 307.94 (d, <sup>2</sup>J<sub>CP</sub> = 21.6 Hz, Ru=C<sub>α</sub>) ppm.

**Synthesis of complex [RuCl(=C(OMe)CH=CPh<sub>2</sub>)(PPh<sub>3</sub>)(κ<sup>3</sup>-N,N,N-pybox)][PF<sub>6</sub>] (**5**).** A solution of *trans*-[RuCl<sub>2</sub>(PPh<sub>3</sub>)(κ<sup>3</sup>-N,N,N-pybox)] (**2a**) (0.651 g, 1 mmol), NaPF<sub>6</sub> (0.840 g, 5 mmol) and

(4) (a) Park, S. B.; Nishiyama, H.; Itoh, Y. *Chem. Commun.* **1994**, 1315–1316. (b) Hua, X.; Shang, M.; Lappin, A. G. *Inorg. Chem.* **1997**, *36*, 3735–3740. (c) Doyle, M. P.; Peterson, C. S.; Zhou, Q.-L.; Nishiyama, H. *Chem. Commun.* **1997**, 211–212. (d) Nishiyama, H.; Itoh, Y.; Sugiyama, H.; Motoyama, Y. *Chem. Commun.* **1997**, 1863. (e) Motoyama, Y.; Murata, K.; Kurihara, O.; Naitoh, T.; Aoki, K.; Nishiyama, H. *Organometallics* **1998**, *17*, 1251–1253.

## Scheme 1

**Table 1.** Crystallographic Data for Complexes **3** and **4b**

	<b>3</b>	<b>4b</b>
empirical formula	C <sub>35</sub> H <sub>38</sub> N <sub>3</sub> Cl <sub>2</sub> O <sub>2</sub> PRu·CHCl <sub>3</sub>	C <sub>50</sub> H <sub>48</sub> ClF <sub>6</sub> N <sub>3</sub> O <sub>2</sub> PRu·THF
fw	854.99	1107.48
<i>T</i> (°C)	20(2)	20(2)
wavelength (Å)	0.710 73	0.710 73
space group	<i>P</i> 2 <sub>1</sub> 2 <sub>1</sub> 2 <sub>1</sub> (No. 19)	<i>P</i> 2 <sub>1</sub> 2 <sub>1</sub> 2 <sub>1</sub> (No. 19)
<i>a</i> , Å	12.772(6)	14.79(3)
<i>b</i> , Å	15.208(5)	16.254(8)
<i>c</i> , Å	19.601(7)	22.917(18)
<i>Z</i>	4	4
<i>V</i> , Å <sup>3</sup>	3807(3)	5509(12)
$\rho_{\text{calcd}}$ , g cm <sup>-3</sup>	1.490	1.335
$\mu$ , cm <sup>-1</sup>	8.41	4.54
R1 [ <i>I</i> > 2 $\sigma$ ( <i>I</i> )] <sup>a</sup>	0.0565	0.0545
wR2 [ <i>I</i> > 2 $\sigma$ ( <i>I</i> )]	0.0944	0.1381

$$^a \text{R1} = \sum(F_o - |F_c|) / \sum F_o; \text{wR2} = [\sum \omega(F_o^2 - F_c^2) / \sum \omega(F_o^2)]^{1/2}.$$

HC≡CC(OH)Ph<sub>2</sub> (1.040 g, 5 mmol) in 30 mL of MeOH was stirred at room temperature for 12 h. The solvent was then removed under vacuum, and the solid residue was extracted with dichloromethane and filtered. The resulting solution was then concentrated to ca. 5 mL, and 20 mL of a mixture hexane/diethyl ether (3/2) was added, yielding a red solid which was washed with diethyl ether (2 × 20 mL) and vacuum-dried. Yield 52% (0.481 g). IR (KBr, cm<sup>-1</sup>)  $\nu$  842 (PF<sub>6</sub><sup>-</sup>). Conductivity (acetone 20 °C;  $\Omega^{-1}$  cm<sup>2</sup> mol<sup>-1</sup>) 127. <sup>31</sup>P{<sup>1</sup>H} NMR (CDCl<sub>3</sub>)  $\delta$  39.80 (s) ppm; <sup>1</sup>H NMR (CDCl<sub>3</sub>)  $\delta$  3.45 and 3.81 (m, 2H each one, OCH<sub>2</sub>), 3.70 (s, 3H, OMe), 4.66 and 4.91 (m, 2H each one, NCH<sub>2</sub>), 6.44–7.95 (m, 29H, Ph, C<sub>5</sub>H<sub>3</sub>N and =CH) ppm.

**X-ray Diffraction Studies.** Data collection, crystal, and refinement parameters are collected in Table 1. Mo K $\alpha$  radiation was used with a graphite crystal monochromator on an Enraf-Nonius CAD4 single-crystal diffractometer ( $\lambda = 0.710 73$  Å). The unit cell parameters were obtained from the least-squares fit of 25 reflections (with  $\theta$  between 6° and 14° for **3**, and between 12° and 16° for **4b**). Data were collected with the  $\omega$ -2 $\theta$  scan technique and a variable scan rate, with a maximum scan time of 60 s per reflection. The intensity of the primary beam was checked throughout the data collection by monitoring three standard reflections every 60 min. The final drift correction factors were between 0.98 and 1.06 for **3**, and between 0.99 and 1.05 for **4b**. On all

reflections, profile analysis was performed;<sup>5</sup> 3277 reflections were observed with  $I > 2\sigma(I)$  for **3** and 3883 for **4b**. Lorentz and polarization corrections were applied and the data were reduced to  $F_o^2$  values. The structures were solved by Patterson methods using the program DIRDIF.<sup>6</sup> Isotropic least-squares refinement on  $F^2$  was made using SHELXL97.<sup>7</sup> At this stage semiempirical absorption correction was applied using XABS2.<sup>8</sup> The relative maximum and minimum transmission factors were, respectively, 1 and 0.0563 for **3**, and 1 and 0.40 for **4b**. During the final stages of the refinement on  $F^2$ , the positional parameters and the anisotropic thermal parameters of the non H-atoms were refined. All non-hydrogen atoms were anisotropically refined. All hydrogen atoms were located by Fourier synthesis and isotropically refined.

**Complex 3.** The function minimized was  $[(\sum \omega(F_o^2 - F_c^2) / \sum \omega(F_o^2))]^{1/2}$  where  $\omega = 1/[\sigma^2(F_o^2) + (0.0203P)^2 + 5.1625P]$  with  $\sigma(F_o)$  from counting statistics and  $P = (\text{Max}(F_o^2, 0) + 2F_c^2)/3$ . The final difference Fourier map showed no peaks higher than 0.617 e Å<sup>-3</sup> nor deeper than -0.451 e Å<sup>-3</sup>.

**Complex 4b.** The function minimized was  $[(\sum \omega(F_o^2 - F_c^2) / \sum \omega(F_o^2))]^{1/2}$  where  $\omega = 1/[\sigma^2(F_o^2) + (0.096P)^2]$  with  $\sigma(F_o)$  from counting statistics and  $P = (\text{Max}(F_o^2, 0) + 2F_c^2)/3$ . The final difference Fourier map showed no peaks higher than 0.916 e Å<sup>-3</sup> nor deeper than -1.097 e Å<sup>-3</sup>.

The crystallographic plots were made with the EUCLID package.<sup>9</sup> Atomic scattering factors were taken from the *International Tables for X-ray Crystallography*.<sup>10</sup> Geometrical calculations were made with PARST.<sup>11</sup> All calculations were made at the University of Oviedo on the Scientific Computer Center and X-ray group VAX and Alpha-AXP computers.

- (5) (a) Lehman, M. S.; Larsen, F. K. *Acta Crystallogr., Sect. A* **1974**, *30*, 580. (b) Grant, D. F.; Gabe, E. J. *J. Appl. Crystallogr.* **1978**, *11*, 114.
- (6) Beurskens, P. T.; Admiraall, G.; Beurskens, G.; Bosman, W. P.; García-Granda, S.; Gould, R. O.; Smits, J. M. M.; Smykalla, C. *The DIRDIF Program System*; Technical Report; Crystallographic Laboratory, University of Nijmegen: Nijmegen, The Netherlands, 1992.
- (7) Sheldrick, G. M. *SHELXL97: Program for the Refinement of Crystal Structures*; University of Göttingen: Göttingen, Germany, 1997.
- (8) Parkin, S.; Moezzi, B.; Hope, H. *J. Appl. Crystallogr.* **1995**, *28*, 53.
- (9) Spek, A. L. *The EUCLID Package*. In *Computational Crystallography*; Sayre, D., Ed.; Clarendon Press: Oxford, UK, 1982; p 528.
- (10) *International Tables for X-ray Crystallography*; Kynoch Press: Birmingham, UK, 1974; Vol. IV.
- (11) Nardelli, M. *Comput. Chem.* **1983**, *7*, 95.



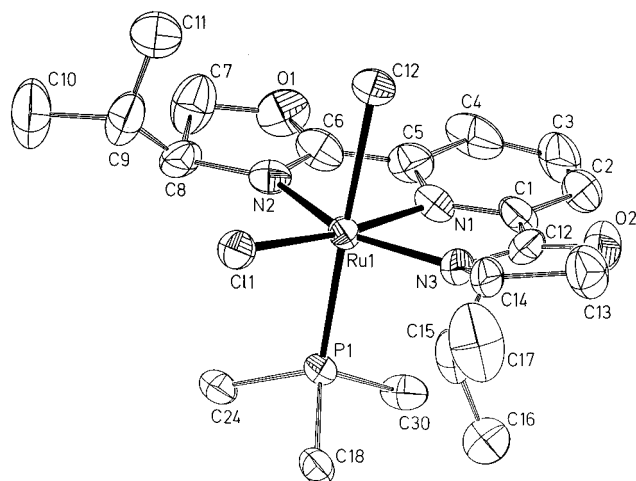


**Figure 1.** ORTEP view of the structure of *cis*-[RuCl<sub>2</sub>(PPh<sub>3</sub>){κ<sup>3</sup>-*N,N,N*-(*SS*)-*iPr*-pybox}] (**3**).

## Results and Discussion

**Synthesis of Complexes *trans*-[RuCl<sub>2</sub>(PPh<sub>3</sub>){κ<sup>3</sup>-*N,N,N*-pybox}] (**2a**) and *trans*- and *cis*-[RuCl<sub>2</sub>(PPh<sub>3</sub>){κ<sup>3</sup>-*N,N,N*-(*SS*)-*iPr*-pybox}] (**2b**, **3**).** We have used as readily available precursors the achiral complex *trans*-[RuCl<sub>2</sub>(η<sup>2</sup>-H<sub>2</sub>C=CH<sub>2</sub>){κ<sup>3</sup>-*N,N,N*-pybox}] (**1a**)<sup>3b</sup> and the chiral analogue *trans*-[RuCl<sub>2</sub>(η<sup>2</sup>-H<sub>2</sub>C=CH<sub>2</sub>){κ<sup>3</sup>-*N,N,N*-(*SS*)-*iPr*-pybox}] (**1b**), containing the enantiomerically pure 2,6-bis[4'-(*S*)-isopropylloxazolin-2'-yl]-pyridine ligand.<sup>3a</sup> Thus, the stereoselective displacement of the ethylene ligand on **1a** by triphenylphosphine gives, after 12 h of heating at 50 °C in dichloromethane, complex *trans*-[RuCl<sub>2</sub>(PPh<sub>3</sub>){κ<sup>3</sup>-*N,N,N*-pybox}] (**2a**) (69% yield) (Scheme 1). As expected, the <sup>31</sup>P{<sup>1</sup>H} NMR spectrum shows a singlet phosphorus resonance at δ 46.48 ppm. The stereochemistry of **2a** is readily determined on the basis of its <sup>1</sup>H NMR spectrum which exhibits two triplet signals for the methylene protons (δ 3.47 and 4.72 ppm, *J*<sub>HH</sub> = 9.8 Hz) in accordance with a C<sub>2</sub> symmetric structure. A similar substitution of ethylene by PPh<sub>3</sub> takes also place in complex **1b** but in contrast the reaction is accomplished in only 1 h to yield *trans*-[RuCl<sub>2</sub>(PPh<sub>3</sub>){κ<sup>3</sup>-*N,N,N*-(*SS*)-*iPr*-pybox}] (**2b**) (64% yield) (Scheme 1). It is apparent that the presence of the two bulky *iPr* groups promotes the higher reactivity of **1b** compared to **1a**. The <sup>1</sup>H NMR spectrum of **2b** shows only two sets of methyl resonances as expected for a chiral complex with C<sub>2</sub> symmetry [δ 0.30 ppm (d, *J*<sub>HH</sub> = 7.1 Hz) and 0.55 ppm (d, *J*<sub>HH</sub> = 6.6 Hz)]. The phosphorus resonance of the PPh<sub>3</sub> ligand appears, in the <sup>31</sup>P{<sup>1</sup>H} NMR spectrum, as a singlet at δ 38.11 ppm.

Although complexes **2a,b** are stable at room temperature both in the solid state or in solution, the chiral complex **2b** slowly isomerizes (ca. 24 h) in acetone at 50 °C to generate the thermodynamically stable *cis* isomer **3** in almost quantitatively yield (Scheme 1). The structure of **3** has been confirmed by X-ray crystallography (Figure 1). Table 2 collects selected bond distances and bond angles. The structural parameters found can be compared to those reported for other six-coordinate ruthenium(II) complexes containing the (*SS*)-*iPr*-pybox ligand: *trans*-[Ru(OAc)<sub>2</sub>(CO){κ<sup>3</sup>-*N,N,N*-(*SS*)-*iPr*-pybox}]<sup>3b</sup>, *cis*- and *trans*-[RuCl(py)<sub>2</sub>{κ<sup>3</sup>-*N,N,N*-(*SS*)-*iPr*-pybox}][PF<sub>6</sub>]<sup>4b</sup>, *trans*-[RuCl<sub>2</sub>(py){κ<sup>3</sup>-*N,N,N*-(*SS*)-*iPr*-pybox}]<sup>4b</sup>, and *trans*-[RuCl<sub>2</sub>(η<sup>2</sup>-acrolein){κ<sup>3</sup>-*N,N,N*-(*SS*)-*iPr*-pybox}]<sup>4d</sup>. Remarkably, although the pybox skeleton is almost planar, one of the oxazoline rings shows a puckering due to the steric interactions between the PPh<sub>3</sub> ligand and its *iPr* substituent. The <sup>1</sup>H NMR spectrum of **3** is in accord with the loss of C<sub>2</sub> symmetry showing four doublet resonances

**Table 2.** Selected Bond Distances (Å) and Bond Angles (deg) for Complex **3**

Bond Distances			
Ru—Cl(1)	2.428(2)	C(6)—O(1)	1.342(11)
Ru—Cl(2)	2.465(3)	O(1)—C(7)	1.440(11)
Ru—P(1)	2.308(2)	C(7)—C(8)	1.525(12)
Ru—N(1)	1.972(7)	C(8)—N(2)	1.485(11)
Ru—N(2)	2.119(6)	C(1)—C(12)	1.421(14)
Ru—N(3)	2.101(7)	N(3)—C(12)	1.310(12)
N(1)—C(1)	1.340(11)	C(12)—O(2)	1.342(11)
N(1)—C(5)	1.351(11)	O(2)—C(13)	1.435(12)
C(1)—C(2)	1.396(13)	C(13)—C(14)	1.558(13)
C(2)—C(3)	1.386(16)	C(14)—N(3)	1.498(11)
C(3)—C(4)	1.374(16)	P(1)—C(30)	1.824(9)
C(4)—C(5)	1.412(14)	P(1)—C(18)	1.830(9)
C(5)—C(6)	1.449(14)	P(1)—C(24)	1.824(9)
N(2)—C(6)	1.272(11)		
Bond Angles			
N(1)—Ru—Cl(1)	172.2(2)	N(1)—C(5)—C(4)	121.4(10)
N(2)—Ru—N(3)	155.8(3)	N(1)—C(1)—C(2)	121.2(10)
Cl(2)—Ru—P(1)	178.32(9)	C(1)—N(1)—C(5)	120.5(8)
N(1)—Ru—Cl(2)	83.6(2)	C(1)—C(2)—C(3)	117.8(10)
N(1)—Ru—P(1)	94.8(2)	C(2)—C(3)—C(4)	122.2(11)
N(1)—Ru—N(2)	77.8(3)	C(3)—C(4)—C(5)	116.8(11)
N(1)—Ru—N(3)	78.2(3)	Ru—N(3)—C(14)	138.1(6)
Ru—P(1)—C(30)	107.7(3)	Ru—N(3)—C(12)	110.4(7)
Ru—P(1)—C(18)	124.4(3)	N(3)—C(2)—O(2)	117.6(10)
Ru—P(1)—C(24)	117.4(3)	C(12)—O(2)—C(13)	106.8(8)
Ru—N(1)—C(1)	119.6(6)	O(2)—C(13)—C(14)	105.5(8)
Ru—N(1)—C(5)	119.6(7)	N(3)—C(14)—C(13)	101.9(8)
Ru—N(2)—C(6)	111.5(6)	N(2)—C(6)—C(5)	120.9(8)
Ru—N(2)—C(8)	142.3(6)	N(1)—C(5)—C(6)	110.1(8)
N(2)—C(6)—O(1)	119.6(9)	N(1)—C(1)—C(12)	110.5(8)
N(2)—C(8)—C(7)	102.6(8)	N(3)—C(12)—C(1)	121.0(9)
C(6)—N(2)—C(8)	106.2(7)		

for the methyl groups which appear at δ -0.12 (*J*<sub>HH</sub> = 6.6 Hz), 0.79 (*J*<sub>HH</sub> = 7.0 Hz), 0.89 (*J*<sub>HH</sub> = 7.2 Hz), and 0.96 (*J*<sub>HH</sub> = 6.6 Hz) ppm. The isomerization process from **2b** to **3** can be explained by taking into account an initial PPh<sub>3</sub> dissociation on **2b**, probably due to the steric hindrance between the triphenylphosphine and both *iPr* groups, to generate the five-coordinate intermediate *trans*-[RuCl<sub>2</sub>{κ<sup>3</sup>-*N,N,N*-(*SS*)-*iPr*-pybox}] which slowly rearranges to the corresponding *cis* isomer. Reoordination of the PPh<sub>3</sub> ligand affords the final complex **3**. An alternative mechanism involving an initial chloride dissociation to yield the cationic intermediate [RuCl(PPh<sub>3</sub>){κ<sup>3</sup>-*N,N,N*-(*SS*)-*iPr*-pybox}]<sup>+</sup> in which the PPh<sub>3</sub> ligand shifts from the equatorial to the axial position cannot be discarded. It is worth mentioning that **3** can be also obtained directly from **1b** by substitution of the ethylene ligand by PPh<sub>3</sub> in methanol as solvent (50 °C, 12 h, 76% yield) (Scheme 1). This result seems to indicate that the *trans*-*cis* isomerization in the pentacoordinated intermediate is clearly favored in a polar media. In contrast, complex **2a** does not isomerize to the corresponding *cis* isomer and is also the only product observed when the ethylene substitution from **1a** takes place in methanol. Thus, we can conclude that the steric interactions between the bulky PPh<sub>3</sub> ligand and the oxazoline ring substituents clearly govern the *cis* or *trans* coordination preference.

**Synthesis and Reactivity of Allenylidene Complexes [RuCl(=C=C=CPh<sub>2</sub>)(PPh<sub>3</sub>){κ<sup>3</sup>-*N,N,N*-pybox}][BF<sub>4</sub>] (**4a**) and [RuCl(=C=C=CPh<sub>2</sub>)(PPh<sub>3</sub>){κ<sup>3</sup>-*N,N,N*-(*SS*)-*iPr*-pybox}][PF<sub>6</sub>] (**4b**).** Ruthenium(II) complexes have proven to be excellent precursors for the stabilization of unsaturated carbene ligands such as vinylidene or allenylidene chains generated from terminal alkynes.<sup>12</sup> Nevertheless, studies concerning the activa-

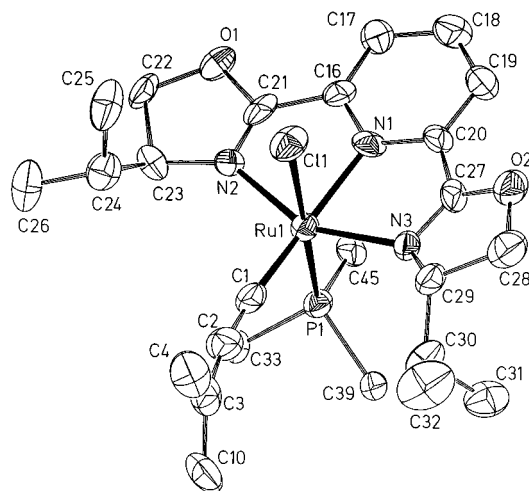


**Figure 2.** ORTEP view of the structure of the cationic part  $[\text{RuCl}(\text{C}=\text{C}=\text{CPh}_2)(\text{PPh}_3)\{\kappa^3\text{-}N,N,N\text{-}(\text{SS})\text{-}i\text{-Pr-pybox}\}]^+$  of complex **4b**.

tion of terminal alkynes by ruthenium(II) derivatives containing terdentate nitrogen ligands are scarce,<sup>13</sup> and to the best of our knowledge only one allenylidene complex, namely  $[\text{Ru}\{\text{C}=\text{C}=\text{C}(\text{Me})\text{Ph}\}(\text{Tp})(\text{dippe})][\text{BPh}_4]$  [Tp = hydrotris(pyrazolyl)-borate; dippe = 1,2-bis(diisopropylphino)ethane], has been reported.<sup>13b</sup> With these precedents in mind we decided to explore the reactivity of **2a,b** and **3** toward propargyl alcohol derivatives since represents one of the most expeditious ways to achieve allenylidene derivatives.<sup>12</sup> Thus, the reaction of complexes **2a,b** with 1,1-diphenyl-2-propyn-1-ol, in the presence of  $\text{AgBF}_4/\text{CH}_2\text{-Cl}_2$  or  $\text{NaPF}_6/\text{MeOH}$  respectively, affords the cationic diphenylallenylidene derivatives **4a,b** (Scheme 1). The  $^{13}\text{C}\{^1\text{H}\}$  NMR data of **4a,b** are in accord with the presence of the cumulene moiety, and can be compared to those reported for other octahedral ruthenium(II) allenylidene derivatives.<sup>14</sup> Significantly, the typical low-field resonance of the carbenic  $\text{Ru}=\text{C}_\alpha$  appears, in the  $^{13}\text{C}\{^1\text{H}\}$  NMR spectra, as a doublet at  $\delta$  306.59 ( $^2J_{\text{CP}} = 22.2$  Hz) (**4a**) and 307.94 ( $^2J_{\text{CP}} = 21.6$  Hz) (**4b**) ppm.

The stereochemistry of **4b** has been confirmed by X-ray crystallography. The molecular structure is shown in Figure 2 and consists of  $[\text{RuCl}(\text{C}=\text{C}=\text{CPh}_2)(\text{PPh}_3)\{\kappa^3\text{-}N,N,N\text{-}(\text{SS})\text{-}i\text{-Pr-pybox}\}]^+$  cations, hexafluorophosphate anions, and one THF molecule of crystallization. Selected bond distances and bond angles are listed in Table 3. The diphenylallenylidene ligand which is located trans to the pyridine ring of the (SS)-i-Pr-pybox ligand, is bound to ruthenium in a nearly linear fashion [ $\text{Ru}-\text{C}(1)-\text{C}(2) = 168(1)^\circ$ ;  $\text{C}(1)-\text{C}(2)-\text{C}(3) = 173(1)^\circ$ ] with bond lengths which can be compared to those reported for other ruthenium allenylidene complexes<sup>14a,c,15</sup> [ $\text{Ru}-\text{C}(1) = 1.86(1)$  Å,  $\text{C}(1)-\text{C}(2) = 1.26(1)$  Å, and  $\text{C}(2)-\text{C}(3) = 1.35(1)$  Å].

**Table 3.** Selected Bond Distances (Å) and Bond Angles (deg) for Complex **4b**

Bond Distances			
Ru-Cl(1)	2.444(4)	C(18)-C(19)	1.356(15)
Ru-C(1)	1.868(11)	C(19)-C(20)	1.389(14)
Ru-P(1)	2.300(4)	C(16)-C(21)	1.484(15)
Ru-N(1)	2.081(8)	C(20)-C(27)	1.502(14)
Ru-N(2)	2.108(8)	N(2)-C(21)	1.274(13)
Ru-N(3)	2.095(8)	C(21)-O(1)	1.354(11)
C(1)-C(2)	1.266(14)	O(1)-C(22)	1.464(14)
C(2)-C(3)	1.353(14)	C(22)-C(23)	1.536(14)
C(3)-C(4)	1.486(17)	C(23)-N(2)	1.467(14)
C(3)-C(10)	1.512(16)	N(3)-C(27)	1.282(12)
N(1)-C(16)	1.363(12)	C(27)-O(2)	1.324(11)
N(1)-C(20)	1.310(12)	O(2)-C(28)	1.460(19)
C(16)-C(17)	1.349(13)	C(28)-C(29)	1.54(2)
C(17)-C(18)	1.421(17)	C(29)-N(3)	1.461(13)
Bond Angles			
N(1)-Ru-Cl(1)	83.9(2)	C(22)-C(23)-N(2)	103.1(9)
N(2)-Ru-N(3)	152.1(3)	N(1)-C(16)-C(17)	121.2(10)
Cl(1)-Ru-P(1)	178.92(10)	C(16)-C(17)-C(18)	119.2(10)
N(1)-Ru-Cl(1)	83.9(2)	C(17)-C(18)-C(19)	118.6(11)
N(1)-Ru-P(1)	95.7(2)	C(18)-C(19)-C(20)	118.9(11)
N(1)-Ru-N(2)	76.5(3)	C(19)-C(20)-N(1)	122.5(10)
N(1)-Ru-N(3)	76.1(3)	Ru-N(3)-C(27)	113.7(6)
Ru-C(1)-C(2)	168.9(10)	Ru-N(3)-C(29)	133.1(7)
C(1)-C(2)-C(3)	173.1(12)	N(3)-C(27)-O(2)	119.5(9)
N(1)-Ru-C(1)	171.9(4)	O(2)-C(28)-C(29)	103.9(11)
Ru-N(1)-C(16)	119.8(7)	C(28)-C(29)-N(3)	103.2(11)
Ru-N(1)-C(20)	120.6(7)	N(3)-C(27)-C(20)	120.6(9)
Ru-N(2)-C(21)	113.3(7)	N(1)-C(20)-C(27)	108.0(9)
Ru-N(2)-C(23)	138.8(7)	N(1)-C(16)-C(21)	107.1(9)
N(2)-C(21)-O(1)	118.6(9)	N(2)-C(21)-C(16)	123.2(9)
C(21)-O(1)-C(22)	104.6(8)	C(2)-C(3)-C(4)	120.0(11)
O(1)-C(22)-C(23)	105.2(8)	C(2)-C(3)-C(10)	117.4(11)

Similarly to complex **3**, the structure of **4b** shows the puckering of one of the five-membered oxazoline rings from the expected planarity. The stereochemistry found for **4b** indicates that a simultaneous isomerization process has occurred, probably on the cationic five-coordinate intermediate  $[\text{RuCl}(\text{PPh}_3)\{\kappa^3\text{-}N,N,N\text{-}(\text{SS})\text{-}i\text{-Pr-pybox}\}][\text{PF}_6]$ . As expected, **4b** can be also obtained starting from the cis isomer **3** in the same reaction conditions (Scheme 1). Since the spectroscopic data of complex **4a** (see Experimental Section) can be compared to those of **4b** a similar stereochemistry is proposed for the former.

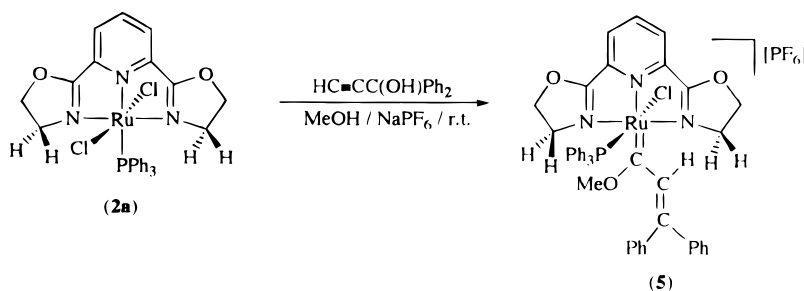
The stability of allenylidene compounds **4a,b** seems to be also governed by the oxazoline-rings substituents. Thus, while **4b** is unreactive toward methanol (it is synthesized in this solvent) complex **4a** reacts with methanol to afford the Fischer type methoxy- $\alpha,\beta$ -unsaturated carbene derivative  $\text{RuCl}\{\text{C}(\text{OMe})\text{CH}=\text{CPh}_2\}(\text{PPh}_3)(\kappa^3\text{-}N,N,N\text{-pybox})[\text{PF}_6]$  (**5**) as it is clearly shown in the reaction of **2a** with 1,1-diphenyl-2-propyn-1-ol and  $\text{NaPF}_6$  in methanol (Scheme 2). The formation of **5** results from the nucleophilic addition of methanol at the  $\text{C}_\alpha$  atom of the unsaturated chain on the initially formed allenylidene complex **4a**. Apparently, the  $\text{C}_\alpha$  atom of the allenylidene chain in the complex **4b** is sterically more protected than in **4a** due to the presence of the bulky isopropyl groups preventing the nucleophilic addition of methanol at this position.

(13) (a) Yang, S. M.; Chan, M. C. W.; Cheung, K. K.; Che, C. M.; Peng, S. M. *Organometallics* **1997**, *16*, 2819–2826. (b) Jiménez Tenorio, M. A.; Jiménez Tenorio, M.; Puerta, M. C.; Valerga, P. *Organometallics* **1997**, *16*, 5528–5535. (c) Takahashi, Y.; Akita, M.; Hikichi, S.; Moro-oka, Y. *Inorg. Chem.* **1998**, *37*, 3186–3194. (d) Slugovc, C.; Mereiter, K.; Schmid, R.; Kirchner, K. *J. Am. Chem. Soc.* **1998**, *120*, 6175–6176. (e) Slugovc, C.; Mauthner, K.; Kacetyl, M.; Mereiter, K.; Schmid, R.; Kirchner, K. *Chem. Eur. J.* **1998**, *4*, 2043–2050 and references therein.

(14) For recent references, see: (a) Touchard, D.; Haquette, P.; Daridor, A.; Romero, A.; Dixneuf, P. H. *Organometallics* **1998**, *17*, 3844–3852. (b) Haquette, P.; Touchard, D.; Toupet, L.; Dixneuf, P. *J. Organomet. Chem.* **1998**, *565*, 63–73. (c) Werner, H.; Grünwald, C.; Steinert, P.; Gevert, O.; Wolf, J. *J. Organomet. Chem.* **1998**, *565*, 231–241. (d) Grünwald, C.; Laubender, M.; Wolf, J.; Werner, H. *J. Chem. Soc., Dalton Trans.* **1998**, 833–839.

(15) For recent references, see: (a) Cadierno, V.; Gamasa, M. P.; Gimeno, J.; González-Cueva, M.; Lastra, E.; Borge, J.; García-Granda, S.; Pérez-Carreño, E. *Organometallics* **1996**, *15*, 2137. (b) Martín, M.; Gevert, O.; Werner, H. *J. Chem. Soc., Dalton Trans.* **1996**, 2275. (c) M. P. Gamasa, J. Gimeno, C. González-Bernardo, J. Borge, S. García-Granda *Organometallics* **1997**, *16*, 2483. (d) Winter, R. F.; Horning, F. M. *Organometallics* **1997**, *16*, 4284. (e) de los Rios, I.; Jiménez-Tenorio, M.; Puerta, M.; C.; Valerga, P. *J. Organomet. Chem.* **1997**, *549*, 221. (f) Bruce, M. I.; Hinterding, P.; Low, P. J.; Skelton, B. W.; White, A. H. *J. Chem. Soc., Dalton Trans.* **1998**, 467.

## Scheme 2



In summary, in this work we report the stereoselective synthesis of *trans*-[RuCl<sub>2</sub>(PPh<sub>3</sub>)(κ<sup>3</sup>-*N,N,N*-pybox)] (**2a**), *cis*-[RuCl<sub>2</sub>(PPh<sub>3</sub>){κ<sup>3</sup>-*N,N,N*-(*SS*)-*i*Pr-pybox}] (**3**), and *trans*-[RuCl<sub>2</sub>(PPh<sub>3</sub>){κ<sup>3</sup>-*N,N,N*-(*SS*)-*i*Pr-pybox}] (**2b**) which are the first phosphine ruthenium(II) complexes containing achiral and chiral pybox ligands. These complexes are precursors of novel cationic allenylidene derivatives [RuCl(=C=C=CPh<sub>2</sub>)(PPh<sub>3</sub>)(κ<sup>3</sup>-*N,N,N*-pybox)][BF<sub>4</sub>] (**4a**) and [RuCl(=C=C=CPh<sub>2</sub>)(PPh<sub>3</sub>){κ<sup>3</sup>-*N,N,N*-(*SS*)-*i*Pr-pybox}][PF<sub>6</sub>] (**4b**). To the best of our knowledge, complex **4b** is the first cumulenylidene complex in which the carbene moiety is attached to a chiral metal fragment. The stability of the chiral allenylidene complex **4b** toward methanol, in contrast to the reactivity of the non chiral complex **4a** which leads to the formation of the methoxy-α,β-unsaturated carbene derivative [RuCl{=C(OMe)CH=CPh<sub>2</sub>}(PPh<sub>3</sub>)(κ<sup>3</sup>-*N,N,N*-

pybox)][PF<sub>6</sub>] (**5**), reveals the steric protection of the isopropyl substituents in the chiral pybox on the C<sub>α</sub> atom of the allenylidene chain. Further studies concerning the synthesis and the reactivity of these type of complexes including other Fischer type α,β-unsaturated carbene derivatives are now in progress.

**Acknowledgment.** This work was supported by the Ministerio de Educación y Cultura of Spain (DGICYT, Projects PB96-0556 and PB96-0558) and the EU (Human Capital Mobility Programme, Project ERBCHRXCT 940501).

**Supporting Information Available:** X-ray crystallographic files, in CIF format, for the structure determinations of **3** and **4b** are available free of charge via the Internet at <http://pubs.acs.org>.

IC9813258